

Simple, soluble bootstrap model with Regge behavior for inclusive reactions*

Robert J. Yaes

Department of Physics, Memorial University of Newfoundland, St. John's, Newfoundland, Canada

(Received 22 April 1974)

We show that a large class of multiperipheral models satisfy the bootstrap integral equation obtained by Krzywicki and Petersson and by Finkelstein and Peccei. We relate the leading-particle distribution directly to the parameters of the multiperipheral model. We present a simple one-dimensional model, closely related to the Chew-Pignotti model, for which the bootstrap equations are exactly soluble and we discuss the properties of the solution. We show how the bootstrap integral equations can be modified to provide a two-component model containing both pionization and diffraction.

I. INTRODUCTION

It is a well-known empirical fact that in production processes, a particle with the same quantum numbers as the projectile tends to retain, on the average, about half the projectile energy. This "leading-particle effect" is responsible for the fact that in the inclusive process $a + b \rightarrow c + X$, there will be an enhancement in the fragmentation region of a if a and c have the same quantum numbers, which is absent if they do not. Such an enhancement is evident, for example, in the data of Albrow *et al.*,¹ for the reaction $p + p \rightarrow p + X$, at the CERN ISR.

Krzywicki and Petersson² have conjectured that the distribution of particles in the fireball recoiling off the leading particle, as a function of the missing mass squared, M^2 , in the fireball rest frame, is the same as the total distribution in the c.m. frame, as a function of the total c.m. energy squared, s . This conjecture has been partially confirmed by the observation³ that in the reaction $p + p \rightarrow p + X$ at NAL, the charged-particle multiplicity in the fireball as a function of M^2 is similar to the total charged multiplicity as a function of s .

Given the leading-particle distribution, the "bootstrap hypothesis" of Krzywicki and Petersson leads to a recursion relation, in the form of an integral equation, for the complete single-particle distribution.^{2,4} The higher-order inclusive distributions,⁴ correlation functions,⁵ and the generating function for the multiplicity moments⁶ can also be determined. The implications of the bootstrap hypothesis were first investigated in detail by Finkelstein and Peccei⁴ in the case where all produced particles are identical and spinless, and we shall limit ourselves to that case in this paper. However, the inclusion of quantum numbers in the model is straightforward.⁷

It has been pointed out⁶ that the results mentioned above tend to indicate that the bootstrap picture

and the multiperipheral picture are equivalent. In Sec. II we shall therefore look in detail at the relationship between the bootstrap models and the multiperipheral models, and we shall see explicitly that for a large class of simple multiperipheral models, the single-particle distribution does satisfy the bootstrap integral equation. In the process we shall obtain an explicit expression for the leading-particle distribution in terms of the parameters of the multiperipheral model. All of the results known for multiperipheral models⁸ can then be directly applied to the bootstrap model. It then becomes clear that the advantage of the bootstrap formulation over the conventional formulation of the multiperipheral model⁹ is that we obtain the inclusive distribution directly from the bootstrap integral equation. Since this equation is most simply formulated in terms of the Feynman scaling variable x rather than the rapidity y , it is best suited to describing the distribution in the fragmentation region where we expect it to be interesting (in the pionization region, as a function of y , the single-particle inclusive distribution is uninteresting since we expect nothing more than a flat plateau).

In Sec. III we shall discuss in detail a simple one-dimensional model, closely related to the classic Chew-Pignotti model,¹⁰ for which the bootstrap equation is exactly soluble. In Sec. IV we shall briefly discuss the way in which a diffractive component can be added to the model. We shall discuss in detail the properties of this two-component bootstrap model in a subsequent paper. In Sec. V we shall offer some speculations as to why even this two-component model may not be adequate.

II. RELATION BETWEEN THE BOOTSTRAP MODEL AND THE MULTIPERIPHERAL MODEL

The single-particle invariant inclusive cross section is given by the expression

$$\frac{d\hat{\sigma}}{dp_1} = \frac{1}{2}(2\pi)^4 \lambda^{-1}(s) \sum_{\pi=1}^{\infty} \frac{1}{(n-1)!} \int dp_2 \cdots dp_n |\langle p_a, p_b | T | p_1, \dots, p_n \rangle|^2 \delta^4 \left(P - \sum_{i=1}^n p_i \right), \tag{2.1}$$

where $P = p_a + p_b$, $P^2 = s$, $dp_i = d^3p_i/2E_i$, $\lambda^{-1}(s)$ is the flux factor and T is the T matrix for the process $p_a + p_b \rightarrow p_1 + \cdots + p_n$. Let us consider a simple multiperipheral-type model. The n -particle T matrix can then be written

$$T_n = \sum_{\pi} D_{n,\pi}, \tag{2.2}$$

where $D_{n,\pi}$ represents the contribution of a single multiperipheral diagram corresponding to a given permutation, π , of the momenta p_1, \dots, p_n . We sum over all $n!$ permutations. The diagram corresponding to the canonical ordering, where π is the identity permutation, I , is given in Fig. 1.

The leading particle is defined to be the particle emitted at the top of the multiperipheral chain (e.g., p_1 in the canonical ordering of Fig. 1). We can define $T_{n,i}$ to be the sum of all n -particle multiperipheral diagrams with particle i the leading particle. In Eq. (2.2), the contribution to $T_{n,i}$ will come from the sum over the subset of permutations that permute the momenta $p_1, \dots, p_{i-1}, p_{i+1}, \dots, p_n$, leaving the leading-particle momentum p_i unchanged. Calling this subset of permutations $\pi'(i)$, we can write Eq. (2.2) as

$$T_n = \sum_i \sum_{\pi'(i)} D_{n,\pi}. \tag{2.3a}$$

$$\sum_{\pi'(i)} D_{n,\pi} = T_{n,i}, \tag{2.3b}$$

so T_n can be written as a sum of $T_{n,i}$,

$$\langle p_a, p_b | T | p_1, \dots, p_n \rangle = \sum_{i=1}^n \langle p_a, p_b | T_i | p_1, \dots, p_n \rangle. \tag{2.4}$$

The term $T_{n,i}$ can be represented by Fig. 2 where the blob represents a sum over all permutations of the outgoing momenta.

Since in multiperipheral models the $D_{n,\pi}$ are assumed to be Q factorizable,¹¹ the dependence on the leading-particle momentum will factor out of each term in Eq. (2.3b) in the same way, as indicated in Fig. 2, and hence out of $T_{n,i}$. The remainder will be the sum over all multiperipheral diagrams that contribute to the blob in Fig. 2. However, the sum of all such diagrams is just the total T matrix for the $(n-1)$ -particle production process,

$$(p_a - p_i) + p_b \rightarrow p_1 + \cdots + p_{i-1} + p_{i+1} + \cdots + p_n.$$

We thus have

$$\langle p_a, p_b | T_i | p_1, \dots, p_n \rangle = f(s, M_i^2, t_i) \langle p_a - p_i, p_b | T | p_1, \dots, p_{i-1}, p_{i+1}, \dots, p_n \rangle, \tag{2.5}$$

where

$$M_i^2 = (p_a + p_b - p_i)^2, \quad t_i = (p_a - p_i)^2. \tag{2.6}$$

It is an essential feature of multiperipheral models that the amplitude vanishes whenever the momentum transfer between adjacent particles becomes large. It is this feature of the model that gives rise to the "strong ordering" and which is responsible for the fact that the major contri-

bution of each of the $D_{n,\pi}$ will be in a different region of phase space. This condition can be assured by requiring that f vanish when the momentum transfer t_i becomes large.

If the model is to satisfy Feynman scaling, f must be a function only of the ratio (s/M_i^2) , not of s and M_i^2 separately. In a simple ABFST (Amati-Bertocchi-Fubini-Stanghellini-Tonin) model, f would in fact depend only on t_i , and

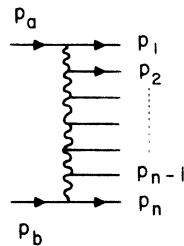


FIG. 1. The n -particle multiperipheral graph for the canonical ordering of the particles.

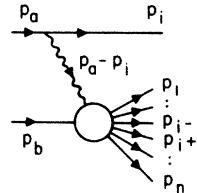


FIG. 2. $T_{n,i}$, the sum over all n -particle multiperipheral graphs where particle i is the leading particle. The blob represents the sum over all permutations of the remaining $n - 1$ particles.

would have the form

$$f(s, M_i^2, t_i) = g/(t_i - m^2). \quad (2.7)$$

In a multi-Regge model, with a single trajectory α , f would have the form

$$f(s, M_i^2, t_i) = \Gamma(t_i) \left(\frac{s}{M_i^2} \right)^{\alpha(t_i)}. \quad (2.8)$$

Here $\Gamma(t_i)$ is a cutoff function that becomes small when t_i becomes large. It is necessary to meet the above-mentioned condition, and, for the moment, shall remain arbitrary. The model can be further simplified by assuming that the trajectory is linear, $\alpha(t_i) = at_i + b$. We shall discuss this type of model in detail in Sec. III.

We thus wish to obtain an expression for the single-particle inclusive distribution for the set of models which satisfy Eqs. (2.4) and (2.5). The fact that, in these models, after the dependence on the leading particle has been removed the remainder is described by the $(n-1)$ -particle T matrix is a restatement of the bootstrap hypothesis from an *exclusive* point of view. We can thus see

that the bootstrap hypothesis is an essential aspect of these multiperipheral models. What we now wish to show explicitly is that these models satisfy the bootstrap integral equation obtained by Krzywicki and Petersson and by Finkelstein and Peccei.

When we substitute Eqs. (2.4) and (2.5) into Eq. (2.1) we make the additional assumption that in calculating the square of the T matrix, cross terms, $T_i T_j$ ($i \neq j$), can be neglected since each of the T_i will contribute mainly to a different region of phase space. The contribution to the single-particle inclusive cross section then divides naturally into two parts: the contribution from $T_{n,1}^2$, where the observed particle is the leading particle, which we shall call $d\hat{\sigma}_L/dp_1$, and the contribution from $\sum_{i \neq 1} T_{n,i}^2$, where the observed particle is nonleading, which we can call $d\hat{\sigma}_N/dp_1$. Therefore,

$$\frac{d\hat{\sigma}}{dp_1} = \frac{d\hat{\sigma}_L}{dp_1} + \frac{d\hat{\sigma}_N}{dp_1} \quad (2.9)$$

and we have immediately for the first term

$$\frac{d\hat{\sigma}_L}{dp_1} = \frac{1}{2}(2\pi)^4 \lambda^{-1}(s) f^2(s, M^2, t) \sum_{n=1}^{\infty} \frac{1}{(n-1)!} \int dp_2 \cdots dp_n |\langle p_a - p_1, p_b | T | p_2, \dots, p_n \rangle|^2 \delta^4 \left(P - p_1 - \sum_{i=2}^n p_i \right), \quad (2.10)$$

where, for simplicity, we have obviously written $M^2 = M_1^2$, $t = t_1$. The sum in Eq. (2.10) is a function of the two invariants, M^2 , the missing mass squared, and t , the "mass" of the exchanged object with momentum $p_a - p_1$. Since the total cross section is defined to be

$$\sigma(s) = \frac{1}{2}(2\pi)^4 \lambda^{-1}(s) \sum_{n=0}^{\infty} \frac{1}{n!} \int dp_1 \cdots dp_n |\langle p_a, p_b | T | p_1, \dots, p_n \rangle|^2 \delta^4 \left(P - \sum_{i=1}^n p_i \right) \quad (2.11)$$

we can write Eq. (2.10) as

$$\frac{d\hat{\sigma}_L}{dp_1} = f^2(s, M^2, t) \frac{\lambda(M^2)}{\lambda(s)} \sigma(t, M^2), \quad (2.12)$$

where

$$\sigma(t, M^2) = \frac{1}{2}(2\pi)^4 \lambda^{-1}(M^2) \sum_{n=1}^{\infty} \frac{1}{(n-1)!} \int dp_2 \cdots dp_n |\langle p_a - p_1, p_b | T | p_2, \dots, p_n \rangle|^2 \delta^4 \left(P - p_1 - \sum_{i=2}^n p_i \right).$$

$\sigma(t, M^2)$ can be thought of as the total cross section for the scattering of a particle with momentum p_b from an off-shell "exchanged object" with momentum $p_a - p_1$. For $t = m^2$ we recover the physical cross section,

$$\sigma(m^2, M^2) = \sigma(M^2). \quad (2.13)$$

Because of the limit on momentum transfer inherent in the multiperipheral model, the exchanged object cannot get too far off-shell, that is, we must have

$$|t| \ll s, M^2. \quad (2.14)$$

It is therefore a reasonable approximation to set

$$\sigma(t, M^2) \cong \sigma(M^2). \quad (2.15)$$

In any event, any t dependence of $\sigma(t, M^2)$ can be approximated by an additional t -dependent factor that could be incorporated in the definition of f , as has been done explicitly for the ABFST model.¹² We therefore have, dividing by $\sigma(s)$ to obtain the inclusive density,

$$\begin{aligned} N_L(p, s) &= \frac{1}{\sigma(s)} \frac{d\hat{\sigma}_L(s)}{dp_1} \\ &= \frac{\lambda(M^2)\sigma(M^2)}{\lambda(s)\sigma(s)} f^2(s, M^2, t). \end{aligned} \quad (2.16)$$

The fact that this type of representation is valid

for the leading-particle distribution in multi-peripheral models has been previously noted.^{13,14} In allowing us to relate the behavior of the inclusive cross sections directly to that of the total cross section this representation has certain interesting consequences, particularly for the

correlation functions.^{14,15}

We must now consider the second term. Since the momenta p_2, \dots, p_n in Eq. (2.1) are dummy variables, the contribution to the inclusive cross section of all of the T_i ($i \neq 1$) will be equal. We can therefore replace $\sum_{i=2}^n T_i^2$ by $(n-1)T_2^2$ and we have

$$\frac{d\hat{\sigma}_N}{dp_1} = \frac{1}{2}(2\pi)^4 \lambda^{-1}(s) \int dp_2 f^2(s, M_2^2, t_2) \sum_{n=2}^{\infty} \frac{1}{(n-2)!} \int dp_3 \cdots dp_n |\langle p_a - p_2, p_b | T | p_1, p_3, \dots, p_n \rangle|^2 \delta^4 \left(P - p_2 - \sum_{i \neq 2} p_i \right). \quad (2.17)$$

Comparing Eq. (2.17) with Eq. (2.1), we see that except for kinematic factors the sum in Eq. (2.17) is just the inclusive cross section, for the process $(p_a - p_2) + p_b \rightarrow p_1 + \text{anything}$, evaluated in the rest frame of the fireball. However, since one line is off-shell, this inclusive cross section will depend on t_2 as well as on M_2^2 , p_1^\parallel , and p_1^\perp . We must therefore once again make an assumption about the off-shell dependence. We can note that if we integrated this inclusive cross section over p_1 we would obtain $\langle n(M_2^2) \rangle \sigma(t_2, M_2^2)$. Hence, if we assume that the off-shell dependence can be factored out of both the inclusive and the total cross sections, this factor must be the same. We will thus assume that if we divide the off-shell inclusive cross section by the appropriate off-shell total cross section, we remove the off-shell dependence and obtain the on-shell inclusive density, $N(\tilde{p}_1, M_2^2)$. Here \tilde{p}_1 is the vector obtained from p_1 by the Lorentz transformation from the c.m. frame to

the rest frame of the fireball. However, from Eq. (2.12), we have

$$f^2(s, M_2^2, t_2) = \frac{\lambda(s)}{\lambda(M_2^2) \sigma(t_2, M_2^2)} \frac{d\hat{\sigma}_L}{dp_2}. \quad (2.18)$$

So Eq. (2.17) becomes

$$\frac{d\hat{\sigma}_N}{dp_1} = \int dp_2 \frac{d\hat{\sigma}_L}{dp_2} N(\tilde{p}_1, M_2^2). \quad (2.19)$$

Adding $d\hat{\sigma}_L/dp_1$ to obtain the total inclusive cross section and dividing by $\sigma(s)$ to get the inclusive density, we finally obtain

$$N(p, s) = N_L(p, s) + \int dp' N_L(p', s) N(\tilde{p}, M'^2). \quad (2.20)$$

This, however, is just the Krzywicki-Petersson-Finkelstein-Peccei bootstrap equation.

It is also clear that if we integrate over the leading-particle distribution, we have

$$\int \frac{d\hat{\sigma}_L}{dp_1} dp_1 = \frac{1}{2}(2\pi)^4 \lambda^{-1}(s) \sum_{n=1}^{\infty} \frac{1}{(n-1)!} \int dp_1 \cdots dp_n |\langle p_a, p_b | T_1 | p_1, \dots, p_n \rangle|^2 \delta^4 \left(P - \sum_{i=1}^n p_i \right). \quad (2.21)$$

Now, since all the momenta are dummy variables we can replace $T_{n,1}^2$ by

$$\frac{1}{n} \sum_{i=1}^n T_{n,i}^2 \text{ or by } \frac{1}{n} T_n^2.$$

Comparing the result with Eq. (2.11), we see that we obtain just the total cross section. Hence N_L must satisfy the normalization condition

$$\int dp N_L(p, s) = 1. \quad (2.22)$$

This is just a restatement of the fact that there is one and only one leading particle in each event.

Finkelstein and Peccei⁴ and also Jengo, Krzywicki, and Petersson⁶ have shown explicitly that the solution of the bootstrap equation must satisfy the energy-momentum-conservation sum rules. We can now see why that must be the case, since we have obtained the bootstrap equation,

for a set of models, by writing the inclusive cross section as a sum over exclusive cross sections, each of which explicitly contains an energy-momentum-conservation δ function. It was, in fact, by a similar technique that these sum rules were originally derived.¹⁶

If we iterate Eq. (2.20),

$$N = N_L + N_L N_L + N_L N_L N_L + \cdots, \quad (2.23)$$

its physical interpretation becomes clear. Each term in the sum represents a sum of multiperipheral diagrams where the observed particle occupies a given position in the multiperipheral chain. The leading-particle distribution, N_L , is given by the sum of all diagrams where the observed particle is the first particle emitted on the chain. The second term in Eq. (2.23) represents the sum of all diagrams where the ob-

served particle is the *second* particle on the multiperipheral chain, and so on. Thus, asymptotically, each term in Eq. (2.23) represents the sum over an infinite number of multiperipheral graphs, but, of course, at any finite energy, the number of graphs that contribute is limited. We can thus see that the difference between the bootstrap formulation of the multiperipheral model and the usual formulation is in the order in which the diagrams are summed.

It is also interesting to note that using the same arguments, we can obtain a recursion relation, similar to Eq. (2.20) for the semi-inclusive distributions.¹⁷ $N^{(n)}(p, s)$ is the semi-inclusive density¹⁸ defined to be

$$N^{(n)}(p, s) = \frac{1}{\sigma^{(n)}} \frac{d\hat{\sigma}^{(n)}}{dp_1}, \quad (2.24)$$

where $\sigma^{(n)}$ is the n -particle total cross section and $d\hat{\sigma}^{(n)}/dp_1$ is the semi-inclusive cross section, the contribution to the inclusive cross section from states of definite multiplicity. If we define $N_L^{(n)}$ in the same way, it can be easily seen that, analogously to Eq. (2.20), we have

$$N^{(n)}(p, s) = N_L^{(n)}(p, s) + \int dp' N_L^{(n)}(p', s) N^{(n-1)}(\tilde{p}, M'^2). \quad (2.25)$$

Since in events of fixed multiplicity we also have one and only one leading particle, we must have for all n

$$\int dp N_L^{(n)}(p, s) = 1, \quad (2.26)$$

but, instead of Eq. (2.16),

$$N_L^{(n)}(p, s) = \frac{\lambda(M^2)\sigma^{(n-1)}(M^2)}{\lambda(s)\sigma^{(n)}(s)} f^2(s, M^2, t). \quad (2.27)$$

III. A SIMPLE, SOLUBLE MODEL

We now wish to consider a simple multi-Regge model in more detail. For simplicity we shall assume that there is no dependence on the Toller angles and that there is only one trajectory, $\alpha(t)$, which can be assumed to be linear, $\alpha(t) = at + b$. In this case, the T matrix is assumed to have the form

$$\langle p_a, p_b | T | p_1, \dots, p_n \rangle = g \prod_{i=1}^{n-1} \Gamma(t_i) (s_{i, i+1})^{\alpha(t_i)}, \quad (3.1)$$

where

$$s_{i, j} = (p_i + p_j)^2, \quad t_i = (p_a - p_1 - p_2 - \dots - p_i)^2. \quad (3.2)$$

From energy-momentum conservation, we must

have $t_{n-1} = (p_b - p_n)^2$. The cutoff function $\Gamma(t_i)$ is such that it is approximately constant and equal to the coupling constant g when t_i is small, but it vanishes when t_i becomes large. This factor is necessary to ensure that the amplitude vanish unless all of the momentum transfers are small. The presence of this factor is merely a reflection of the fact that Regge theory determines only the asymptotic behavior of the model, that is, its behavior in that region of phase space where each of the $s_{i, i+1}$ is large and each of t_i is small. It is a basic assumption of the model that the major contribution to the amplitude comes from this region of phase space and it is the presence of the $\Gamma(t_i)$ factors that ensures that this will indeed be the case.

As we have previously noted in Sec. II and discussed in detail elsewhere,¹⁴ if the T matrix is given by Eq. (3.1), then it can be easily seen that the leading-particle distribution is given by Eqs. (2.8) and (2.16). Since $\lambda(s) \cong s$ for large s , we have for this model

$$N_L(p, s) = \Gamma^2(t) \left(\frac{s}{M^2} \right)^{2\alpha(t)-1} \frac{\sigma(M^2)}{\sigma(s)}. \quad (3.3)$$

To say anything more about the shape of the leading-particle distribution, we must make an assumption about the asymptotic behavior of the total cross section. The simplest assumption is that the total cross section behaves like a power of s . Because of the Froissart bound, this power must be negative,

$$\sigma(s) \sim s^{-\epsilon}, \quad (3.4)$$

so that we would have

$$N_L(p, s) = \Gamma^2(t) \left(\frac{s}{M^2} \right)^{2\alpha(t) + \epsilon - 1}. \quad (3.5)$$

Hence, we conclude that if the cross section falls like $s^{-\epsilon}$, the intercept of the effective trajectory that determines the shape of the leading-particle distribution (and, hence, through the bootstrap equation, the shape of the whole inclusive distribution) is increased by $\frac{1}{2}\epsilon$ over what it would have been if the cross section were constant,

$$\alpha_{\text{eff}}(t) = \alpha(t) + \frac{1}{2}\epsilon. \quad (3.6)$$

The model can be further simplified by integrating over transverse momenta to obtain a one-dimensional model essentially equivalent to the Chew-Pignotti model. Since

$$t = m_a^2(1-x) + m^2 + (p^{\perp 2} + m^2)/x \quad (3.7)$$

in the limit $p^{\perp 2} \gg p^{\perp 2}, m^2$, it is clear that N_L in Eq. (3.5) satisfies Feynman scaling, and, therefore, so must N . We can therefore define

$$f(x) = \int \frac{d^2 p^\perp}{2(2\pi)^3} N(x, p^\perp), \tag{3.8}$$

$$g(x) = \int \frac{d^2 p^\perp}{2(2\pi)^3} N_L(x, p^\perp).$$

The normalization condition Eq. (2.22) then becomes

$$\int_0^1 \frac{dx}{x} g(x) dx = 1, \tag{3.9}$$

which can only be satisfied if

$$g(0) = 0. \tag{3.10}$$

We have taken $g(x)$ to be the distribution of the leading particle associated with the projectile. We must therefore have asymptotically

$$g(x) = 0, \quad x < 0. \tag{3.11}$$

The probability that the leading particle is traveling backward must be zero since it would involve a momentum transfer t of the same order of magnitude as s . However, there must also be a "lagging particle" associated with the target with distribution $\bar{g}(x)$. If the target and projectile are identical, we must have

$$\bar{g}(x) = g(-x). \tag{3.12}$$

We could also define the symmetrical distribution

$$\bar{g}(x) = g(x) + \bar{g}(x), \tag{3.13}$$

and of course for the region $x \geq 0$, $\bar{g} = g$. Hence, if we restrict ourselves to this region, it does not matter whether we consider g or \bar{g} as the leading-particle distribution. Finkelstein and Peccei seem to have taken the latter case. Finkelstein and Peccei have shown⁴ that if we restrict ourselves to the region $x \geq 0$ and integrate Eq. (2.20) over p^\perp , we obtain the one-dimensional bootstrap equation

$$f(x) = g(x) + \int_0^{1-x} \frac{dy}{y} g(y) f\left(\frac{x}{1-y}\right). \tag{3.14}$$

If the target and projectile particles are identical, we can obtain f for $x \leq 0$ from the symmetry of f ,

$$f(x) = f(-x). \tag{3.15}$$

If they were not identical, then for $x \leq 0$ we would have

$$f(x) = \bar{g}(x) + \int_{-1-x}^0 \frac{dy}{|y|} g(y) f\left(\frac{x}{1-|y|}\right). \tag{3.16}$$

It is clear that when Eq. (3.12) holds, Eq. (3.16) leads to Eq. (3.15).

Hence, the simple case where the target and projectile are distinct but all produced particles are identical can be dealt with without using the multichannel formalism of Kronenfeld and Peccei.⁷

For $x > 0$, $f(x)$ is determined by the leading-particle distribution $g(x)$, and for $x < 0$ by the lagging-particle distribution $\bar{g}(x)$. If we insist that $f(x)$ be continuous at $x = 0$ there would be a self-consistency condition that $g(x)$ and $\bar{g}(x)$ must satisfy. For simplicity, we shall consider only the case where the projectile and target are identical, below.

If N_L is given by Eq. (3.5), it is clear that we can integrate over p^\perp and write

$$g(x) = \gamma(x)(1-x)^{1-2\alpha}. \tag{3.17}$$

Here α is an average value for the effective Regge trajectory. $\gamma(x)$ is a cutoff function which must satisfy

$$\gamma(0) = 0 \tag{3.18}$$

in order that Eq. (3.10) be satisfied.¹⁹ The behavior of $\gamma(x)$ for small x is determined by that of $\Gamma^2(t)$ for large t since for small x , $t \sim 1/x$. In particular, if $\Gamma^2(t)$ falls off like $1/t$ then $\gamma(x) \sim x$ for small x . Since the cutoff function is arbitrary except for Eq. (3.18) and the requirement that it be a smooth function of x , we should therefore choose it so as to make the model as simple as possible. Let us therefore consider the case where we choose $\gamma(x) = cx$. The constant c is determined by the normalization condition and we would then have

$$g(x) = (\beta + 1)x(1-x)^\beta, \quad \beta = (1 - 2\alpha). \tag{3.19}$$

Once we have chosen the cutoff function, the model depends on two parameters, α and the parameter ϵ that determines the behavior of the total cross section. In the Chew-Pignotti model there are also two parameters, the average Regge trajectory α_0 and the coupling constant g . From Eq. (3.6) it is clear that we have $\alpha = \alpha_0 + \frac{1}{2}\epsilon$. However, we also have the Chew-Pignotti relation,

$$-\epsilon = 2\alpha_0 - 2 + g^2, \tag{3.20}$$

whence

$$\alpha = 1 - \frac{1}{2}g^2. \tag{3.21}$$

Hence we obtain the peculiar result that the effective average trajectory α , which determines the shape of the inclusive distribution, depends only on the coupling constant g^2 and not on the average exchanged trajectory α_0 . The parameter α_0 affects only the asymptotic behavior of the total cross section.

It is a simple matter to see that with $g(x)$ given by Eq. (3.19), the bootstrap equation is exactly soluble. Substituting Eq. (3.19) into Eq. (3.14), we can see by inspection that a solution of the equation is

$$f(x) = (\beta + 1)(1-x)^\beta.$$

It is obvious that this solution satisfies three conditions that must be satisfied by any solution:

$$f(x) \geq g(x), \quad 0 \leq x \leq 1 \quad (3.23a)$$

$$\lim_{x \rightarrow 1} [f(x) - g(x)]/f(x) \rightarrow 0, \quad (3.23b)$$

$$\int_0^1 f(x) dx = 1. \quad (3.23c)$$

Equation (3.23c) is just the energy-momentum-conservation sum rule.

We can consider the properties of the solution in three different cases:

$$\beta > 0, \quad \alpha < \frac{1}{2} \quad (3.24a)$$

$$\beta = 0, \quad \alpha = \frac{1}{2} \quad (3.24b)$$

$$-1 < \beta < 0, \quad \frac{1}{2} < \alpha < 1. \quad (3.24c)$$

The second case, $\alpha = \frac{1}{2}$, $\beta = 0$, has already been dealt with by Finkelstein and Peccei. We have $g(x) = x$, $f(x) = 1$ and the single-particle density is constant over the whole range $0 \leq x \leq 1$. In the first case, $\beta > 0$, it is clear that the function $f(x) = (\beta + 1)(1 - x)^\beta$ will have a maximum at $x = 0$ and will go to zero at $x = 1$. Such behavior of the single-particle inclusive density can be called "pionization-like" (Fig. 3). As β becomes larger, the peak at $x = 0$ becomes sharper.

In the third case, $-1 < \beta < 0$, $\frac{1}{2} < \alpha < 1$, $f(x)$ will have a minimum at $x = 0$ and will become infinite at $x = 1$. We can call such behavior "diffraction-like" (Fig. 4). It has, in fact, been noted that for sufficiently small values of the coupling constant, diffraction-like behavior can be manifested by a multiperipheral model.²⁰ We should note that the

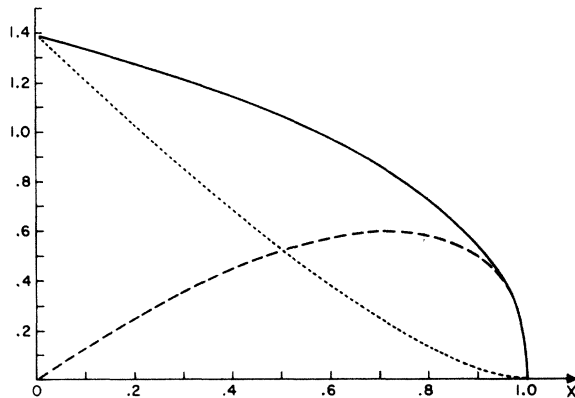


FIG. 3. "Pionization-like" behavior of the bootstrap model. The single-particle inclusive distribution (solid line), $f(x) = (\beta + 1)(1 - x)^\beta$, the leading particle distribution, $g(x) = (\beta + 1)x(1 - x)^\beta$ (dashed line), the nonleading particle distribution, $h(x) = f(x) - g(x) = (\beta + 1)(1 - x)^{\beta + 1}$ (dotted line) for the choice of parameter, $\beta = 0.4$ corresponding to $\alpha = 0.3$.

case $\alpha = 1$, which from Eq. (3.21) would correspond to a vanishingly small coupling constant, is not allowed since in this case, neither $f(x)$ nor $g(x)$ is integrable, and, consequently, neither the normalization condition (3.9) nor the energy-momentum sum rule (3.23c) could be satisfied. However, as we shall see below, this difficulty could be overcome, at any finite energy, by dealing more realistically with the behavior of $g(x)$ in the region $x \cong 1$.

The nonleading-particle distribution, $h(x) = f(x) - g(x)$, also has Regge behavior near $x = 1$,

$$h(x) = (\beta + 1)(1 - x)^{\beta + 1}, \quad (3.25)$$

but the trajectory intercept is decreased by $\frac{1}{2}$. Hence, even for $-1 < \beta < 0$ where $f(x)$ is diffraction-like, $h(x)$ will be pionization-like. Hence, in this model, the diffraction peak is due *entirely* to the leading-particle distribution, and if the leading particle is removed from each event it will disappear, even though the nonleading particles are also produced by the exchange of a trajectory with an $\alpha > \frac{1}{2}$. This is a consequence of energy-momentum conservation.

Finally, we should emphasize that our approach is somewhat different from those of previous authors.^{24, 5} They have obtained $f(x)$, or constraints on it, from experiment or from Mueller-Regge analysis. The bootstrap equation was then used to obtain information about the leading-particle distribution, multiparticle distributions, and correlation functions. On the other hand, we have assumed that the leading-particle distribution is given directly by the model and the bootstrap equation is used to obtain additional information from it.

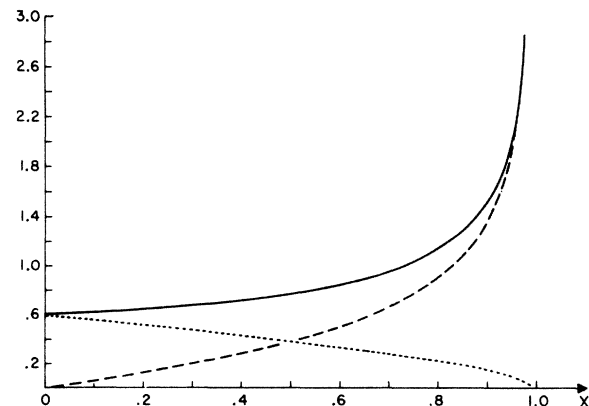


FIG. 4. "Diffraction-like" behavior of the bootstrap model. $f(x)$ (solid line), $g(x)$ (dashed line), and $h(x)$ (dotted line) for $\beta = -0.4$, $\alpha = 0.7$.

IV. TWO-COMPONENT BOOTSTRAP MODEL

The model we have just discussed allows the exchange of only a single Regge trajectory. To make the model more realistic we would have to include the contribution that the exchange of lower-lying trajectories makes to the leading-particle distribution, so that instead of Eq. (3.3) we would have

$$N_L(p, s) = \sum_i \Gamma_i^2(t) \left(\frac{s}{M^2}\right)^{\alpha_i(t)-1} \frac{\sigma(M^2)}{\sigma(s)}. \quad (4.1)$$

The behavior of the single-particle distribution near $x=1$ will still be determined by the leading trajectory but the behavior near $x=0$ will be more complicated. In particular, it would be possible to obtain the correct Mueller-Regge behavior in the pionization region, which can *not* be done in the model with only a single trajectory.²¹

It is evident from the shape of the inclusive proton distribution at the CERN ISR¹ and from analysis of the multiplicity and correlation data²² that both diffraction and pionization components are present in the real world. These two components can be obtained in the context of the multiperipheral model by allowing the exchange of the Pomeron as well as at least one "ordinary" trajectory.

If the total cross section is asymptotically constant and the Pomeron is a simple pole, its intercept must be exactly one. In that case, to avoid a violation of the Froissart bound, the Finkelstein-Kajantie theorem²³ requires that there be no more than one Pomeron in a multiperipheral chain. Two-component multiperipheral models of this type have been constructed by Kajantie and Ruuskanen²⁴ and by Jones.²⁵ Multiperipheral diagrams containing no Pomeron contribute to the pionization component. Diagrams with a Pomeron at the end of the multiperipheral chain contribute to single-fireball diffractive events and diagrams with a Pomeron somewhere in the middle contribute to two-fireball diffractive events (Fig. 5).

Another point of view is the "weakly recurrent Pomeron" picture of Chew and collaborators,²⁶ who assume that there is a "bare Pomeron" with intercept slightly less than one, which can be exchanged an arbitrary number of times. However, if the intercept is very close to one, the coupling constant must be very small. This suggests that the amplitude can be expanded in powers of the Pomeron coupling constant. The first-order term would correspond to the two-component model with only one Pomeron exchanged. Higher-order terms do not seem to be important even at ISR energies.

In bootstrap language, we can say that the lead-

ing particle can be produced either by the exchange of a Pomeron or an "ordinary" trajectory. The leading-particle distribution is thus a sum of two terms,

$$N_L = N_{L\alpha} + N_{LP}, \quad (4.2)$$

where $N_{L\alpha}$ is the leading-particle distribution arising from the exchange of an "ordinary" trajectory and N_{LP} , from the exchange of a Pomeron. If the leading particle is produced by Pomeron exchange, then the remaining fireball can contain only ordinary Regge trajectories. On the other hand, if the leading particle is produced by the exchange of an "ordinary" trajectory, the remaining fireball can contain a Pomeron and its amplitude will have the same form as that for the whole process. In analogy with Eq. (2.20), we should have an equation of the form

$$N(p, s) = N_{L\alpha}(p, s) + N_{LP}(p, s) + \int dp' N_{L\alpha}(p', s) N(\tilde{p}, M'^2) + \int dp' N_{LP}(p', s) N_{\alpha}(\tilde{p}, M'^2). \quad (4.3)$$

Here N_{α} is the distribution for a one-component model, with just an ordinary trajectory, of the type discussed in Sec. III. It should therefore satisfy an equation of the form

$$N_{\alpha}(p, s) = \bar{N}_{L\alpha}(p, s) + \int dp' \bar{N}_{L\alpha}(p', s) N_{\alpha}(\tilde{p}, M'^2). \quad (4.4)$$

We should emphasize that it is not necessarily the

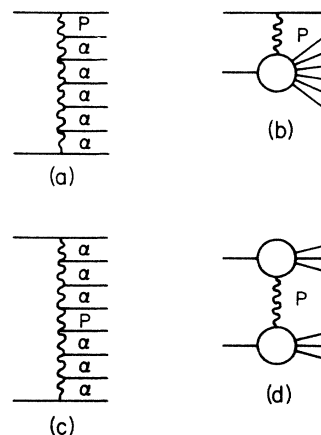


FIG. 5. (a) A multiperipheral diagram that contains a single Pomeron at the end of the multiperipheral chain that describes a single-fireball event (b). A similar diagram can of course be drawn with the Pomeron at the other end of the chain. (c) A diagram with a Pomeron in the middle of the multiperipheral chain that describes a two-fireball diffractive event (d).

case that $N_{L\alpha} = \bar{N}_{L\alpha}$. We have seen that the behavior of the leading-particle distribution depends on the behavior of the total cross section as well as on the exchanged trajectory, and the total cross section could have different asymptotic behavior in the one- and two-component models. We shall discuss the two-component bootstrap model in detail in a subsequent paper.

V. A THREE-COMPONENT MODEL?

Our results for the behavior of $g(x)$ in Sec. III depended on the power-law behavior of the total cross section, $\sigma(s) \sim s^{-\epsilon}$ over the whole range of s . This leads us to the conclusion that a "Pomeron" with $\alpha = \alpha_0 + \frac{1}{2}\epsilon = 1$ is not compatible with the model since the integrals of both f and g would diverge at the upper limit, and neither the normalization condition nor the energy-momentum sum rule can be satisfied. The same conclusion would follow if we tried to incorporate such a "Pomeron" in a two-component model.

A closer look, however, will disclose a flaw in the argument. The $s^{-\epsilon}$ behavior of the total cross section is only the *asymptotic* behavior and cannot persist at low s . In particular, $\sigma(s)$ must vanish as $s \rightarrow 0$ and the phase space for the reaction vanishes. More to the point, as fixed s , $\sigma(M^2)$ does not behave like $(M^2)^{-\epsilon}$ at small M^2 . If we assume that the Pomeron-particle total cross sections will behave, as a function of M^2 , roughly like a particle-particle total cross section as a function of s , the situation would be described roughly by Fig. 6. For M^2 greater than some M_0^2 (around 10 GeV²), the Pomeron-proton total cross

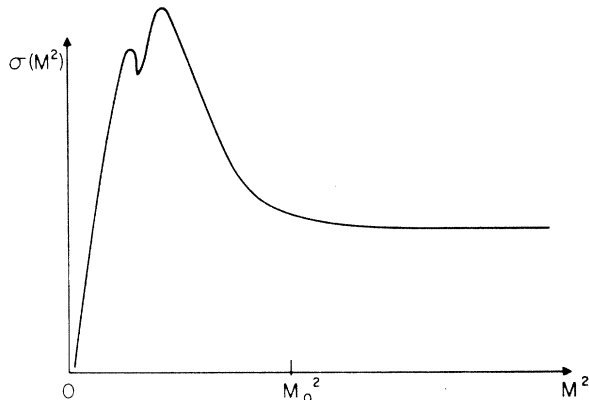


FIG. 6. A rough sketch of how the Pomeron-particle total cross section can be expected to look if its behavior is similar to that of a particle-particle total cross section. For $M^2 > M_0^2$ the cross section can be assumed to be approximately constant. For $M^2 < M_0^2$ the behavior of the cross section is dominated by nonleading Regge trajectories, direct-channel resonances, and phase-space effects.

section is itself dominated by Pomeron exchange and the total cross section is approximately constant (another way of saying that the inclusive cross section is described by the triple-Pomeron term). If we let M^2 become smaller than M_0^2 , the contribution from nonleading Regge trajectories will begin to dominate. As M^2 becomes smaller still, the cross section must be described in terms of direct-channel resonances and a triple-Regge description of the inclusive cross section will no longer be appropriate. Finally, as M^2 approaches the proton mass, phase-space effects dominate and the cross section must vanish as the phase space available for the reaction vanishes. The distinction between the two cases, $M^2 < M_0^2$ and $M^2 > M_0^2$, is just the distinction between "low-mass diffraction" and "high-mass diffraction" proposed by Harari and Rabinovici.²⁷

Hence, for x in the diffraction peak and $x < x_0$,

$$x_0 = \left(1 - \frac{M_0^2}{s}\right), \quad (5.1)$$

the behavior

$$f(x) \sim g(x) \sim (1-x)^{-1} \quad (5.2)$$

is valid. For $x > x_0$, Feynman scaling no longer holds but it is clear that for any fixed finite s both $f(x)$ and $g(x)$ remain finite as $x \rightarrow 1$ and therefore both f and g are integrable. The resolution at the CERN ISR is, of course, not good enough to detect resonance behavior in the diffraction peak.²⁸ However, at NAL the difference between high-mass diffraction and low-mass diffraction can be detected.²⁹ If the resolution could be improved still further, we might expect the diffraction peak to look like Fig. 7. If we assume that the Pomeron-proton total cross section depends only on M^2 and not on s , we could obtain information from lower-energy experiments where low-mass diffraction occupies a greater fraction of the x plot.

If low-mass diffraction is, in fact, dominated by direct-channel resonances, then each resonance will decay into a small fixed number of particles. Hence, independent of energy, low-mass diffraction will contribute only to a small number of topological cross sections, σ_n , with n less than some fixed number n_0 . We can also argue that with a Pomeron at 1, low-mass diffraction contributes a constant to the total cross section.

Consider the inclusive cross section for the particle recoiling off the fireball, integrated over the transverse momentum, in a low-mass diffraction event. It is clear from our previous argument that with a Pomeron exactly at 1, we have

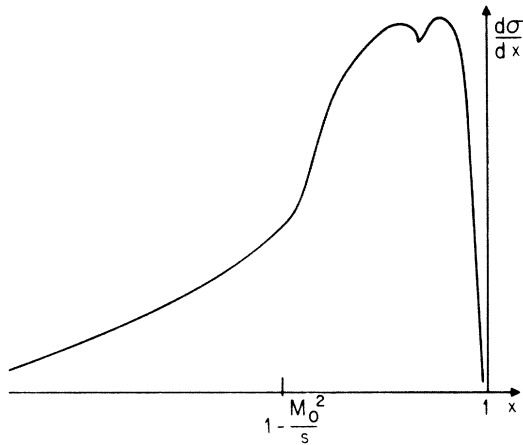


FIG. 7. The behavior of the diffraction peak in the region $x \approx 1$ if our assumptions about the Pomeron-particle total cross section are valid. The $(1-x)^{-1}$ behavior is valid only for $x < (1 - M_0^2/s)$. For any fixed finite s , the inclusive cross section remains finite over the whole range of x . The nonscaling region, $x > (1 - M_0^2/s)$, is the region of low-mass diffraction.

$$\frac{d\hat{\sigma}}{dx} \cong (1-x)^{-1} \sigma(M^2). \quad (5.3)$$

The region of validity for low-mass diffraction is

$$(1 - M_0^2/s) < x < 1. \quad (5.4)$$

The integral of the inclusive cross section over any region of phase space gives the product of the contribution of that region to the total cross section and the average multiplicity in that region. From energy-momentum conservation, we know that there can be only one particle with $x > \frac{1}{2}$. Hence, integrating $d\sigma/dx$ over the low-mass diffraction region will give the total cross section for low-mass diffraction, σ_L (actually, we should multiply by 2 since we will get an additional, equal contribution to low-mass diffraction from the region near $x = -1$). Using Eq. (5.3) and the fact that $M^2 = s(1-x)$, and that in this region $dx/x \cong dx$, we have

$$\begin{aligned} \sigma_L &= \int_{1 - M_0^2/s}^1 (1-x)^{-1} \sigma[s(1-x)] dx \\ &= \int_0^{M_0^2} \sigma(M^2) \frac{dM^2}{M^2}, \end{aligned} \quad (5.5)$$

which is independent of s and finite as long as $\sigma(M^2) \rightarrow 0$ as $M^2 \rightarrow 0$.

In high-mass diffraction, on the other hand, the fireball is described by a multiperipheral model, so the multiplicity in the fireball behaves like $\langle n(M^2) \rangle \sim \ln M^2$. Since $M^2 = s(1-x)$, at any fixed x for the recoiling particle, $\langle n(x) \rangle \sim \ln s$. Hence, integrating over x to get the total multiplicity for

high-mass diffraction, we get $\langle n \rangle \sim \ln s$.

We must thus look at the two components as seen by Le Bellac³⁰ and Van Hove²² in a slightly different way. The component that consists of fixed, low-multiplicity topological cross sections, σ_n ($n < n_0$), and hence has fixed multiplicity, $\langle n \rangle \sim \text{constant}$, is low-mass diffraction. The short-range-correlation component with $\langle n \rangle \sim \ln s$ is the sum of both the pionization component and the high-mass diffraction components. It is the interference of the low-mass diffraction with the sum of the other two components that produces the behavior $f_2 \sim \ln^2 s$.

The bootstrap model, even with high-mass diffraction, is still a short-range-correlation model, although we would expect the correlation length to be larger than in a pure pionization model. We would therefore expect the correlation function, $C(x, 0)$, between the leading particle at x at the end of the multiperipheral chain and a particle at $x = 0$ in the center of the chain to vanish in the scaling limit. On the other hand, when the leading particle is in the low-mass diffraction region, $x \approx 1$, we expect all the decay products of the low-mass fireball to have large negative longitudinal momenta in the c.m. frame and we would expect no particles at $x = 0$. Therefore we would expect $C(x, 0)$ to become negative in the low-mass diffraction region.

The correlation function $C(x, 0)$ between the leading proton and a particle in the $x \approx 0$ region ($\theta = 90^\circ$) has been measured by Albrow *et al.*³¹ Their data are consistent with $C(x, 0) = 0$ for $0.55 \leq x \leq 0.9$, as we would expect. For $x > 0.9$, $C(x, 0)$ falls off sharply, giving a large negative correlation, which is also in qualitative agreement with our expectations. It also seems to be the case that this falloff is less sharp at higher energies where low-mass diffraction makes up a smaller fraction of the total diffractive cross section.

VI. DISCUSSION

We have clarified the relationship between multiperipheral models and bootstrap models by showing explicitly that any model that satisfies Eqs. (2.4) and (2.5) also satisfies the bootstrap integral equation. Since f can be any function of its arguments, provided that it vanishes at large momentum transfer, a large class of models is included. We have had to assume that off-shell effects and the contribution from cross terms can be neglected, but such assumptions are usually made to make models of this type tractable. One can say that it is an alternative statement of the bootstrap hypothesis to say that if you cut the top line off of

a multiperipheral diagram, the remainder is still a multiperipheral diagram.

The bootstrap equation can be a useful phenomenological tool or an interesting theoretical laboratory for testing out simple ideas. As an example of the latter use, we have presented a simple one-dimensional model, closely related to the Chew-Pignotti model. Our model differs from the Chew-Pignotti model only in that we must specify a high-momentum-transfer cutoff function to uniquely determine the leading-particle distribution. Once such a cutoff function is specified, the inclusive distribution depends on a single parameter, the effective Regge trajectory, which depends only on the Chew-Pignotti coupling constant. The average exchanged Regge trajectory parameter affects only the asymptotic behavior of the total cross section.

For the simplest possible cutoff function, the model is exactly soluble, displaying behavior characteristic of pionization for $\alpha < \frac{1}{2}$ and of diffraction for $\alpha > \frac{1}{2}$. While a different cutoff function would change the shape of the inclusive distribution somewhat, it would not qualitatively change the pionization-like or diffraction-like behavior. The behavior of the model with different cutoff

functions or when more than one Regge trajectory is included would have to be investigated numerically.

Since the real world contains both pionization and diffraction, we have seen how the bootstrap equations can be modified to produce a two-component model. This leads to a set of two coupled integral equations whose properties we shall discuss in a subsequent paper. We have also seen that if we take the bootstrap hypothesis literally, it is an inescapable conclusion that we must also distinguish between low-mass diffraction and high-mass diffraction. We must do so because the multiperipheral model is an asymptotic model and can only describe the behavior of the fireball if its mass is large. For a low-mass fireball, the multiperipheral model is not applicable. Its properties must be determined from lower-energy experiments and inserted in the model by hand.

ACKNOWLEDGMENTS

The author is grateful for valuable conversations with Professor J. Finkelstein, Professor K. Kajantie, Professor S. Pinsky, Professor T. T. Gien, and Professor R. D. Murphy.

*Work supported in part by the National Research Council of Canada.

¹M. G. Albrow *et al.* (CERN-Holland-Lancaster-Manchester Collaboration), Nucl. Phys. **B54**, 6 (1973). See also M. G. Albrow *et al.*, papers presented at the International Conference on New Results from High Energy Experiments, Vanderbilt Univ., 1973 (unpublished) and at the Second Aix-en-Provence International Conference on Elementary Particles, 1973 (unpublished). (The leading-particle effect is indicated by the broad maximum in the proton distribution around $x = 0.5$ to 0.6 . It is present at conventional accelerator energies and in all production processes. The presence of an additional sharp peak near $x = 1$ indicates the presence of diffraction and the need for a two-component model.)

²A. Krzywicki and B. Petersson, Phys. Rev. D **6**, 924 (1972).

³S. J. Barish *et al.*, Phys. Rev. Lett. **31**, 1080 (1973). (See also L. Foà, rapporteur's talk at the Second Aix-en-Provence International Conference on Elementary Particles, 1973 (unpublished) [CERN report (unpublished)]; J. Whitmore, Phys. Rep. **10C**, 273 (1974).)

⁴J. Finkelstein and R. D. Peccei, Phys. Rev. D **6**, 2606 (1972).

⁵J. Finkelstein, Phys. Rev. D **8**, 977 (1973).

⁶R. Jengo, A. Krzywicki, and B. Petersson, Nucl. Phys. **B65**, 319 (1973).

⁷R. Kronenfeld and R. D. Peccei, Phys. Rev. D **7**, 1556 (1973).

⁸See, for example, W. R. Frazer *et al.*, Rev. Mod. Phys. **44**, 284 (1972).

⁹We refrain from using the term "multiperipheral bootstrap model" since this expression has already been used in a quite different context (see Ref. 10).

¹⁰G. F. Chew and A. Pignotti, Phys. Rev. **176**, 2112 (1968).

¹¹See, for example, M. Toller, in lectures given at the International Summer Institute on Theoretical Physics, Kaiserslautern, Germany 1972, CERN Report No. Ref. TH. 1530-CERN (unpublished).

¹²M. Bishari, Nucl. Phys. **B48**, 325 (1972).

¹³H. Satz, in *Proceedings of the Amsterdam International Conference on Elementary Particles, 1971*, edited by A. G. Tenner and M. Veltman (North-Holland, Amsterdam, 1972).

¹⁴R. J. Yaes, Phys. Rev. D **7**, 2161 (1973).

¹⁵R. J. Yaes, Nuovo Cimento Lett. **4**, 611 (1972).

¹⁶C. E. DeTar, D. Z. Freedman, and G. Veneziano, Phys. Rev. D **4**, 906 (1971).

¹⁷Z. Koba, H. B. Nielsen, and P. Olesen, Phys. Lett. **38B**, 25 (1972); Nucl. Phys. **40B**, 317 (1972).

¹⁸See, for example, R. J. Yaes, Nuovo Cimento Lett. **8**, 365 (1973).

¹⁹Given Eq. (3.7), one might try a function of the form $(1-x)^{(a+b/x)}$ instead of Eq. (3.17) for $g(x)$. However, it is easy to see that in this case the limit of $g(x)$ as $x \rightarrow 0$ would be e^{-b} , so a cutoff function would still be necessary to obtain the correct behavior at $x = 0$. (The author is grateful to Professor R. D. Murphy for pointing this out.)

²⁰J. Steinhoff, report, McGill University, 1973 (unpublished).

- ²¹The author is particularly grateful to Professor J. Finkelstein and Professor S. Pinsky for discussions on this point. It has, in fact, been shown that the n -channel multiperipheral model and the Mueller-Regge model are equivalent [S. S. Pinsky, D. R. Snider, and G. H. Thomas, *Phys. Lett.* **47B**, 505 (1973)].
- ²²L. Van Hove, *Phys. Lett.* **43B**, 65 (1973); A. Białas, K. Fiałkowski, and K. Zalewski, *Nucl. Phys.* **B48**, 237 (1972).
- ²³J. Finkelstein and K. Kajantie, *Nuovo Cimento* **56A**, 659 (1968).
- ²⁴K. Kajantie and P. V. Ruuskanen, *Phys. Lett.* **45B**, 181 (1973). [See also E. H. de Groot, K. Kajantie, and P. V. Ruuskanen, *Nucl. Phys.* **B71**, 241 (1974).]
- ²⁵S. T. Jones, *Phys. Rev. D* **7**, 197 (1973).
- ²⁶G. F. Chew, LBL Report No. LBL-2174 (unpublished); M. Bishari, G. F. Chew, and J. Koplik, *Nucl. Phys.* **B72**, 61 (1974); M. Bishari and J. Koplik, *ibid.* **B72**, 93 (1974).
- ²⁷H. Harari and E. Rabinovici, Weizmann Institute Report No. WIS 73/41 Ph. (unpublished).
- ²⁸The author is grateful for members of the CERN-Holland-Lancaster-Manchester Collaboration, particularly Dr. M. G. Albrow and Dr. B. Bošnjaković, for conversations concerning the details of their experiment.
- ²⁹J. M. Chapman *et al.*, *Phys. Rev. Lett.* **32**, 257 (1974).
- ³⁰M. Le Bellac, *Phys. Lett.* **37B**, 413 (1971).
- ³¹M. G. Albrow *et al.*, *Phys. Lett.* **44B**, 518 (1973).

Neutral-current effects in elastic electron-nucleon scattering

E. Reya and K. Schilcher

Institut für Physik, Universität Mainz, 6500 Mainz, West Germany

(Received 19 March 1974)

Parity-violating effects are studied in considerable detail for elastic electron-nucleon scattering. Based on a unified Weinberg gauge model properly generalized to include nonstrange hadrons, we derive and discuss corrections to the Rosenbluth formula, and left-right asymmetries of longitudinally polarized electrons as well as nucleons. Any dependence of electron-nucleon scattering on the longitudinal polarization would be evidence of parity violation. The size of such neutral-current effects in general differs from that naively expected on purely dimensional grounds and strongly depends on the nucleon target used.

I. INTRODUCTION

Unified gauge theories of weak and electromagnetic interactions¹ yield striking predictions for leptonic and semileptonic processes.² The main emphasis has for obvious reasons so far been put on neutrino-induced reactions. For electron-induced processes the effects of the neutral weak boson (the Z^0 boson) are in general of order $(G/e^2)q^2$, where q^2 is the momentum transfer squared and G is the weak Fermi coupling constant. With the advent of the new generation of accelerators and electron-nucleon storage rings,³ this neutral weak current could lead to observable effects relative to the electromagnetic background. Possibly high-precision intermediate-energy experiments searching, e.g., for parity violation in elastic electron-nucleon scattering could also yield information on the existence of neutral weak currents.

In this paper we delineate and discuss in considerable detail effects of the Z^0 boson on elastic electron-nucleon scattering. Because of the sharp falloff of the electromagnetic form factors, this

reaction is not the best choice for studying such effects. On the other hand, the fundamental importance of elastic electron-nucleon scattering and, parallel to it, the complete lack of understanding of the q^2 behavior of the form factors warrant a detailed investigation of the effects of weak neutral currents. We find corrections to the Rosenbluth formula and parity-violating effects⁴ in longitudinal electron (or nucleon) polarization experiments to be about one order of magnitude smaller than present experimental accuracy, which leaves hope that some of these effects will be observable in the not too distant future. The feasibility of high-energy experiments with longitudinally polarized electrons and unpolarized protons at the future colliding electron-proton beam machines (for example, EPIC and SPEAR) has been recently discussed.⁵

Any dependence of electron-nucleon scattering on the longitudinal polarization of the electrons (or nucleons) would be direct evidence of parity violation. Naively, these effects are expected to be of order Gq^2/e^2 . Detailed calculations, however, show that this simple picture generally